Proceedings of The Institute of Acoustics

ACOUSTIC TECHNIQUES FOR UNDERWATER SEDIMENT TRANSPORT STUDIES

P. D. Thorne

Institute of Oceanographic Sciences
Bidston Observatory, Birkenhead, Merseyside. L43 7RA

ABSTRACT

The application of acoustic techniques in marine sediment transport research is an area of expanding interest, as the movement of sediments is of concern to sedimentologists, hydraulic engineers, oceanographers, and many other disciplines. Acoustic techniques are being applied to measure water velocity profiles using acoustic doppler devices. Acoustic backscattering and attenuation measurements have been used to monitor suspended sediments. The movement of sandbanks is being measured using acoustic bedform monitors, and the detection of the surficial movement of bed-load sand transport by acoustic impedance changes near the bed surface has been applied. The present paper describes the development of a nonintrusive, rapidly responding, continuously recording acoustic system to obtain field measurements of:-

(i) the initiation of sediment bed-load transport,
(ii) the mass of moving material,
(iii) the size distribution of the mobile particles.

The technique utilises the acoustic self generated noise (SGN) arising from the interparticle collisions of mobile sedimentary material. A laboratory and marine study of this sediment noise with a theoretical description of its probable origin is investigated.

INTRODUCTION

In recent years the use of acoustics to measure current flow and sediment transport rates has become an area of increasing activity [1-4]. The work described here is concerned with measuring gravel transport by monitoring the acoustic noise generated by the interparticle collisions of moving sediment.

The classical technique for monitoring the bedload transport of coarse sedimentary materials has been to deploy a box or tray sampler onto the bed and simply collect mobile material. The limitations and difficulties of this technique have been previously discussed [5,6], and include flow interference, lack of temporal resolution, variable efficiency, disruption of the bed, and other problems specific to particular samplers. To obviate some of these difficulties alternative approaches have been investigated to monitor bedload transport. The possibility of using sidescan sonar to track transponding pebbles has been explored [7], radioactive labelling of gravel particles has been utilised [8], and electromagnetic detection of ferrite loaded pebbles has been applied [9]. An approach which has commanded more attention has been the application of passive acoustic devices to detect gravel movement by measuring the acoustic self generated noise, SGN, arising from the interparticle collisions as bedload transport takes place. The use of a hydrophone to monitor sediment transport is attractive because high temporal resolution

measurements can be obtained without significantly disturbing the flow structure or the state of the seabed, conditions difficult to achieve using conventional techniques. The application of this method is investigated in the present paper.

A number of exploratory field experiments have been conducted by previous investigators [10-16]. However, due to a number of reasons only limited success was achieved. The slow progress has been due in part to insufficient knowledge of the spectral structure, signal level, and physical factors which govern the SGN. Furthermore, no theoretical description of the origins of the acoustic noise had been attempted and this lack of understanding has impeded developments. The deficiency of information has led to ineffectual acoustic systems being designed, which have usually been tested without adequate independent assessment of bedload transport, and therefore the validity of this approach had not been examined in the field with any degree of exactitude. Some limited laboratory studies have been conducted [14,17,18] to provide information on the SGN, and these have indicated that mass transport may be linearly related to acoustic intensity, and the SGN spectrum should be a function of particle size, however, no successful marine application of these studies has been published.

The work described here, firstly, reports a series of laboratory experiments on SGN under conditions where experimental parameters could be varied, and the influence on the acoustic signal investigated. Secondly, an attempt has been made to explain the observations within the theoretical framework of solid body radiation [19]. Finally, the results of a field deployment where this technique has been utilised to monitor bedload gravel transport is reported.

LABORATORY MEASUREMENTS

A selection of measurements on the SGN arising from the interparticle collisions of agitated marine sediments, ranging in type from medium sand, to coarse gravel, are presented. Attention is focussed upon the spectral content of the SGN, and the relationship between the quantity of material present and the total rms signal level.

The instrumentation employed is shown in figure 1. Sediments were agitated in a vertical wooden drum 1m in diameter and 0.5m deep, this rotated about a horizontal axis, and was totally submerged underwater in a tank 3m x 2m x 2m. The front of the drum was open, thereby allowing hydrophones to be placed at any position inside the drum while material was being agitated. The output from the hydrophones was fed into a low noise amplifier, through a 1-600kHz bandpass filter, and in parallel into a rms signal level detector and a spectrum analyser. These results were digitised, fed into a mini-computer, and acoustic pressure levels computed. These SGN observations were taken under conditions where the agitated sediments radiated into the limited volume of the tank, and therefore measurements were conducted in a reverberant environment. This results in a highly complex field containing nodal and antinodal regions, these produce pressure fluctuations at the hydrophone

location which are superimposed on the acoustic spectral signature of the source. To achieve free-field estimates of the source characteristics both spatial [20,21] and frequency [22] averaging were employed, to obtain a reliable description of the effective free-field SGN spectrum. The freefield rms pressure level $P_{FF}(f)_{rms}$, at range R is approximately given by [23].

$$P_{FF}(f)_{rms} = \sqrt{[(A/16\pi R^2)\langle p(f)^2\rangle]} \quad (1)$$

where $\langle P(f)^2\rangle$ is the mean square pressure averaged in time, both spatially and with frequency, and A is the chamber absorption coefficient. Further instrumentation details, and discussions on measurements in a reverberant environment have been presented in a preliminary study using artificial sediments [24].

Initially a series of measurements on the effective free-field spectral characteristics of the SGN were conducted on agitated sediment samples, having an equivalent sphere diameter ranging from 0.3-25mm. The results for 500g of material, with a rotation speed of $0.3ms^{-1}$, and at a range of 30cm from the source (for consistency with ref 24 and the field data) are shown in figure 2. The measurements show the SGN to be composed of bandlimit noise, with a steadily increasing frequency range over which significant contributions to the spectrum occur as particle diameter is reduced. The effect of varying the mass of agitated material, interparticle collision speed, and analyser bandwidth on the SGN spectrum was examined, the variations in these parameters on the spectral form was marginal. The amplitude frequency distribution of the spectrum is almost solely determined by particle size. A characteristic frequency was chosen to represent the frequency band over which the acoustic energy was spread by taking the frequency range over which significant spectral pressure levels, SPL, occurred, (for $P(f)>0.1P(f)_m$ where $P(f)_m$ is the maximum SPL in the spectrum) and computing the centroid frequency f_c^m of the spectrum. The results are given by the solid dots in figure 3, where a steady decrease of f_c with increasing particle diameter is observed. Comparison with other studies[c] is also shown. A linear regression (shown by the solid line) on the logarithm of the present gravel data gave,

$$f_c = 209/D^{0.88} \quad (2)$$

where f_c has units of Hertz and D of metres. The mean rms SPL, P_o, was also computed for the spectra of figure 2 and gave

$$P_o = 25.6 \times D^{0.45} \quad (3)$$

P_o has unit of $mPaHz^{-\frac{1}{2}}$. Therefore as a preliminary guide to instrument development, equations (2) and (3) give direction to the frequency response and sensitivity required of an acoustic system to monitor mobile material of

diameter D.

The relationship between the total rms pressure level and the quantity of agitated material was also examined, and the results for 2.4, 4.7, 9.7 and 16.8mm diameter sediments are shown in figure 4. The gradients of the curves g_1, g_2, g_3, g_4 for the particle sizes 2.4, 4.7, 9.7 and 16.8mm respectively are given by

$$g_1 = 0.56 \pm 0.16 \qquad g_2 = 0.71 \pm 0.21$$
$$g_3 = 0.52 \pm 0.16 \qquad g_4 = 0.5 \pm 0.15 \tag{4}$$

An analysis of the variance of the gradients show that at the 90% confidence limits there is no significant difference in gradient. For similar random independent noise sources the total rms pressure, P_T, is given by [25]

$$P_T = \sqrt{\{\sum_{i=1}^{N} P_i^2\}} \approx \sqrt{N}\, P_i \tag{5}$$

where N is the number of sources and P_i are the individual source rms pressure levels. Now it cannot be stated with certainty that $N \propto M$, where M was the mass of material present, because the method of agitation does not guarantee a linear increase in sources with further addition of material, however, if it is supposed $N \propto M$ then P_i should be approximately dependent on $\sqrt{M}$, as is observed in figure 4. The departure of the gradient from the ideal case of 0.5 is probably due to both sampling errors and the agitation technique. The results obtained here are consistant with previous observations [14,17] which also gave $I = CM$, where I is the intensity and C a constant. Again for instrument design purposes, a guide to the expected total rms pressure level in the marine environment would be of the order of 10^2-10^3 mPa when material was mobile.

To summarise this section the SGN spectra are broad in nature, with a steadily increasing frequency range, over which significant SPL occured as particle diameter reduced. The spectral form is relatively insensitive to variables other than particle size, with the spectra observed having a centroid frequency which is inversly dependent on particle diameter. The total acoustic intensity level yields an approximate linear relationship with the mass of agitated material. Furthermore the data presented can be used as a guide for the design of a marine system for monitoring gravel mobility at sea.

THEORY

The origin of the acoustic energy arising from the interparticle collision of impacting bodies, is a function of both the mechanics of the impact itself, and the source of the radiation. Provisionally it was considered possible that the natural modes of vibrations were being excited within the colliding particles, and that this was the mechanism for generating the observed acoustic field. However, results presented by Love [26], show the modal

vibrations of spheres, with the equivalent diameter of the colliding particles, as having a radiation frequency an order of magnitude above the measured centroid frequencies. Furthermore it has been shown [27] that the energy transferred to these natural vibrations is only a fraction of the initial kinetic energy of the particles. An explanation for the observations has been adopted which utilises the theory of rigid body radiation [19]. In this case an impulse is transmitted into the water, by the surface of the gravel particles, as they undergo a rapid velocity change owing to collision. The sound radiated from an accelerated or decelerated sphere has been previously studied [28,29] where it is shown that both a compression and rarefraction wave is generated, by an impulsively accelerated sphere. The problem of the sound radiated by two colliding spheres has been investigated by a number of authors [30,33]. In these studies each sphere was treated as an independent dipole source, and the field radiated by the two sources summed to describe the total sound field. The pressure radiated by each sphere was obtained by the convolution of kirchhoff's [34] impulse solution with the acceleration time history of the sphere during impact. If the assumption is made that the spheres are undergoing an elastic collision then classical Hertzian impact theory can be applied and a description for the acceleration throughout impact obtained [35]. Using the previous work, [32,33] and following the developments of Richard etal [36,38] an approximate farfield solution, for the time history of the acoustic pulse generated by a single sphere undergoing an Hertzian impact acceleration can be shown to be given by,

$$P(r,t,\theta) = \frac{\rho c U a \cos\theta}{2(1+4\delta^4)r}\{(2\delta^2-1)\cos\pi\tau + 2\delta\sin\pi\tau + [(1-2\delta^2)\cos\pi\delta\tau - (2\delta^2+1)\sin\pi\delta\tau]e^{-\pi\delta\tau}\}$$

for $\tau \leq 1$

$$= \frac{\rho c U a \cos\theta}{2(1+4\delta^4)r}\{[(1-2\delta^2)\cos\pi\delta(\tau-1) - (2\delta^2+1)\sin\pi\delta(\tau-1)]e^{-\pi\delta(\tau-1)} + [(1-2\delta^2)\cos\pi\delta\tau - (2\delta^2+1)\sin\pi\delta\tau]e^{-\pi\delta\tau}\}$$

for $\tau > 1$ (6)

where $\tau = t/t_o$ and $\delta = ct_o/\pi a$. t is the retarded time, t_o is the impact duration time of the collision and is given by

$$t_o = 5.843[\rho_o(1-\sigma^2)/E]^{0.4}(a/U^{0.2}) \quad (7)$$

E is Young's modulus, σ Poisson's ratio, ρ_o the density of the spheres, U the impact velocity, a the sphere radius, r the range from the sphere, θ is the impact grazing angle and ρc the acoustic impedence of the fluid. For two impacting spheres the acoustic impulsive waveform from each sphere is

identical but opposite in phase, and these are summed at the field point with due regard given to the relative time delay associated with the different path lengths to the field point. The total field, P_T, is then given by

$$P_T = P(r,\tau,\theta) - P(r,\tau-\tau_d,\theta) \quad (8)$$

where it is recognised that $P(r,\tau-\tau_d,\theta) = 0$ for $\tau < \tau_d$, and τ_d is the time difference. Using equations (6-8) the pressure waveform was computed for the present experimental arrangement and a Fourier transform of the time series waveform taken. The magnitude of the normalised pressure spectrum is compared with the observation taken in the drum and is shown in figure 2. The theoretical spectrum was matched in amplitude to the observed SPL at f_c. It can be observed that the spectrum derived from equations (6-8) broadly covers the same frequency range as observed experimentally, and is centred on a similar frequency band. The oscillation noted in the theoretical spectrum are not observed in the experimental data because both spatial and frequency averaging were employed in collecting the data, due to working in a reverberant environment as discussed, and the pressure at a particular field point, was generated by a number of impacting sources generated randomly in time and space, and not simply arising from two colliding spheres. The computed peak frequency frequency, f_p, in the spectrum is given approximately by

$$f_p \approx 1/1.1t_o \quad (9)$$

for the present case using equation (7) yields

$$f_p \approx 129/D \quad (10)$$

where f has units of Hertz and D of metres. This result is given by the broken line in figure 3 and compares favourably with the data.

It was noted in the 'Laboratory measurements' section that the centroid frequency was relatively insensitive to parameters other than particle diameter. This is displayed in equation 6, since the variable τ is given by t/t_o, and as shown in equation (7), $t_o \propto 1/U^{0.2}$, and therefore there is only a relatively weak dependence of spectral form on impact velocity. Further for constant U, the value of t_o/a remains fixed, and hence δ = constant and τ_d ≈const (for fixed θ), in this case the spectral form does not change but simply shift up and down in frequency with an inverse dependency on particle size.

Although further theoretical developments are necessary, the present analysis does yield the basis for an explanation for the acoustic noise spectrum generated by the interparticle collision of mobile sediments. The results compare favourably with the experimental gravel data, and although the sediment particles were not spherical, the centroid frequency of the significant spectral region, is comparable with the calculated value for the peak frequency, of the acoustic energy generated by the rigid body radiation of colliding spheres.

ACOUSTIC TECHNIQUES FOR UNDERWATER SEDIMENT TRANSPORT STUDIES

FIELD WORK

The aim of taking the marine measurements was to examine the feasibility of using the SGN technique non-intrusively to study with a high temporal resolution, the detailed variability of marine gravel transport, over a period of the order of a second, for record lengths covering a number of hours, and relate the sediment movement to the instantaneous turbulent flow conditions.

The measurements were conducted in the West Solent, as shown in figure 5. The region has a seabed composed of mixed gravel sizes, with an approximate sphere diameter range of 2-32mm. The channel is approximately 4 km wide and the water depth usually less than 20m. Particularly at Spring tides when strong rectilinear flow is observed over ebb and flood tidal cycles, significant gravel transport is observed. Further background details on the area have been presented [39,40]. Data were collected during September 1982 and October/November 1983. A rig instrumented with a lowlight monochrome underwater TV camera, two hydrophones, electromagnetic current meters, and a string of rotary current meters, was deployed from an anchored ship onto the seabed in a water depth close to 15m. A diagram of the rig is shown in figure 6. All measurements were recorded on a shipborne data logging system. The TV camera was mounted at approximately 0.5m above the bed, and continuous video recordings of the state of the bed covering an area 30x30cm^2 directly below the hydrophones was taken. The hydrophones were mounted at 24cm above the bed, the acoustic rms signal levels were sampled at 5Hz and recorded. For a period of 30 minutes when gravel was mobile the ac signal was recorded on tape with a 150kHz bandwidth, and this data used for spectral analysis of the SGN. The turbulent water flow was measured using a 5Hz sampling rate, at 0.3m above the seabed, and within 0.5m of the hydrophones, using the electromagnetic current meters. The current profile for the first 2m above the bed was calculated from 60s averaged values of the rotary current meters. Additional instrumentation details have previously been presented. [41,42,3]

A detailed analysis of the video recording has been conducted to obtain quantitative estimates of gravel transport rates along the seabed, directly below the hydrophones. These estimates were compared with the acoustic intensity levels, and a statistical analysis conducted. The details of an intercomparison between acoustic and visual monitoring of gravel transport has been published, [42] where it was shown that visual estimates of gravel transport and acoustic intensity levels were significantly correlated. The utilisation of the hydrophones calibrated to measure sediment transport rates is considered here.

An example of the results obtained is shown in figure 7. 10s averaged estimates of gravel transport covering 3.6 hrs is presented. Over a 2.3 hrs period where both TV (d) and SGN transport rates (b,c) were calculated the values are the same order of magnitude and the high temporal variability very similar. In fact the acoustic data reveals how variable is the process of coarse sediment transport. The 10s averaged intensity levels have typical values of 3μWm^{-2} giving a pressure level of 2Pa, which although slightly higher than the laboratory results, is compatible with the laboratory

measurements shown in figure 4. A comparison of the accumulative quantity of material moved over the 2.3 hrs period is shown by the solid circles. Both TV and SGN data show a steady transport of material over approximately the first 1.5 hrs and very little movement afterwards. Over the 2.3 hrs the total quantity of material estimated to have been transported by the hydrophones was 2.25 kgm^{-1}, and 1.6 kgm^{-1}, for the TV. These results show that SGN can be used to remotely monitor coarse gravel transport with modest accuracy, and with a temporal resolution which cannot be obtained using the normal bedload samplers.

Attempts have been made to estimate the onset of sediment transport from the acoustic data, the results of this work are shown in figure 8. An analysis of the flow conditions which causes coarse sediment transport has been previously reported [43], where it was found that turbulent bursting events, in this case principally sweep events, were the main mechanism for the movement of material. In figure 8 the square of the flow velocity, U^2, for approximately 2,400 sweep events is compared with the SGN signal level. U^2 rather than U is chosen because for the high Reynold's numbers (R_{*}>500 observed in the present work) Shields [44] curve predicts the threshold of particle movement to be a function U^2. A linear regression on the data gives an intercept with the abscissa of U_c=1.16ms^{-1}, where U_c is taken to be the critical velocity for sediment transport. This value for U_c can be related to the critical friction velocity, U_{*c}, a parameter frequently utilised in the sediment literature to measure the threshold of particle movement, by the Karman-Prandtt equation [45]

$$U = (U_{*}/K) \ln (z/z_o) \qquad (11)$$

where U is the velocity at height z above the bed, U_{*} is the friction velocity, K is von-Karman's constant (0.4) and z_o is the roughness length. In the present work z=0.33m, z_o=0.005m, U=U_c=1.16ms^{-1}, this gives a value of U_{*c}=0.11ms^{-1}. This value for U_{*c} has to be associated with a particular particle size. From spectral analysis of the SGN and T.V. observations (discussed shortly) a value for D ≈0.01m is obtained, another analysis [46] of a broader coverage of the T.V. data gave a mean value for D as 0.017m. Suffice to say that acoustic estimates of U_{*c}, for particles in the range 0.01-0.0017m, yields a value of 0.11ms^{-1}. This value can be compared with previous observations. Other work in the Solent [46] gave a value of U_{*c}=0.07-0.08ms^{-1} (D=0.01-0.02m) and a review on transport measurements [47] showed U_{*c}=0.085-0.12ms^{-1} for the same size range. The acoustic technique for measuring the initiation of sediment transport gives results which are consistent with those obtained in other studies where visual estimates for threshold were employed.

Figure 7(a) shows the flow velocity and included are the threshold for transport, obtained by the acoustic technique (dashed line) and from reference 46 (solid line). It can be seen that it is the bursts in current flow (2) above the thresholds which cause significant sediment movement, while sharp reductions in flow (1) below the threshold cause minimal transport. Towards the end of the time series, near high water, the mean flow reduces below threshold, and transport ceases.

For a thirty minute period while gravel was mobile recordings of the analogue signal were taken. The major transport event in the period was analysed in detail. A spectrum of the SGN taken in the marine environment, with background noise removed, and due allowance made for any modulation in the spectrum by variations in the total acoustic intensity, is shown in Figure 9a. From the particle size distribution shown in Figure 5 and the results presented in Figure 2, the spectrum covers the frequency range consistent with expectations. A comparison with laboratory measurements on a sample with a similar size distribution yielded very similar results [48]. Two techniques of spectral inversion to predict particle size distribution from the acoustic spectrum have been reported [48], and the results of one approach is shown in Figure 9b. The observed particle size distribution of the mobile material when the spectrum was taken is given in Figure 9c. These measurements show that the spectrum can be used to obtain a particle size distribution for the mobile material which is consistent with visual estimates. The spectrum cannot resolve in detail the particle diameters because of the inherent broadband nature of the spectrum for single size samples, however, it can yield useful though limited information on the predominate size of mobile material. Further details on both the laboratory and marine work can be found in reference 48.

DISCUSSION AND CONCLUSION

A laboratory study on the SGN of agitated marine sediments has been reported. The spectrum is broad in nature, even for a very narrow sample size distribution, and behaves as band limited noise. Significant contributions to the spectrum occur at higher frequencies as particle diameter reduces, leading to the centroid of the spectrum having close to an inverse dependency on particle diameter. The overall form and bandwidth of the spectrum is principally governed by particle size, with a relatively weak dependence on collision velocity. Within the uncertainties associated with the gradient of the line for the four different diameter samples examined, a linear relationship between intensity and the mass of gravel agitated was estimated.

An explanation for the frequency range and spectral form of the acoustic noise, generated by multiple interparticle collisions, has been described in terms of rigid body radiation. Detailed analysis [32,33] of this form of radiation has only been carried out for two impacting spheres, and a heuristic approach has been adopted to extrapolate this work to explain the observations in the present study, when many collisions, randomly distributed in time and space, occured.

Field deployment of an instrument package utilising SGN to monitor coarse sediment transport in the marine environment has been described. The SGN measurement of gravel transport yields a temporal resolution which is not obtainable using convention bedload samplers, and has allowed for the first time a detailed intercomparison between the turbulent flow structure, and the sediment response to the turbulence. Acoustic measurement of the initiation of sediment transport was shown to be consistent with previous results, estimates of mass transport rates comparable with visual observation were achieved, and a crude description of the particle size distribution was

obtained. These measurements were taken without significantly interfering with the flow or the bed.

The work reported here is an attempt to describe the physical basis for the SGN and its possible application for improving our understanding of coarse sediment transport processes. Further studies should yield results which are interesting to both acousticians and sedimentologists.

REFERENCES

1. Lhermitte R. J. Geophys Res Vol.88 No.C1 725-742 Jan 20 1983.
2. Young R.A. etal Geophy Res Ltrs 9(3) 175-178 1982.
3. Thorne P.D. etal IOA. Conf on Acoustics and the seabed 395-402 6-8 April 83
4. Lowe R.L. 17th International Conf on Coastal Egn Sidney 215-216, 23-28 March 1980
5. Hubbell D.W. US Geological Survey Water-Supply Paper, N182/G/1748 pp74 1964.
6. Engel P. etal Proc of the Florence Symposium, IAHS Publ No.133 27-31 Jun 81
7. Dyer K.R. etal International Symposium on interrelationships of esturine and continental shelf sedimentation. Bordeaux, France No.7 377-380 9-14 July 1973.
8. Circkmore M.J. etal Proc 13th Coastal Eng Conf Vancouver Vol2 1005-1025 10-14 July 1972.
9. Reid I. etal Sedimentology 31, 269-276 1984.
10. Bedeaus K. etal Proc Int Assoc Sci. Hydrol. Publ.65, 384-390 1963.
11. Tywoniuk N. etal Proc 9th Canadian Hydrology Symposium Ottawa 728-749 1973.
12. Richards K.S. etal Earth Surface Processes Vol.4, 335-346 1979.
13. Anderson M.G. Earth Surface Processes Vol.1 213-217 1976.
14. Jonys C.K. Inland Water Directorate Ontario Scientific Series No66 pp 118 1976.
15. Harden Jones F.R. etal J. Cons int Explor. Mer. 40(1): 53-61 1982.
16. Voglis etal Ultrasonics 100-101 April 1980.
17. Johnson P. etal J. Hydraul. Res. 7(4): 519-540 1969.
18. Millard N.W. IOA Conf on Recent developments in underwater acoustics ARE Portland 31 March-1 April Pap 3.5 8pp 1976.
19. Akay A. J Acoust. Soc. Am. 64(4) Oct 1978.
20. Waterhouse R. J Acoust Soc Am Vol 48 No1 (Part1) 1-5 1970.
21. Ebbing C.E. J. Sound Vib 16(1) 99-118 1971.
22. Chu W.T. J Acoust Soc Am 72(1) 196-199 July 1982.
23. Morse P.M. etal Theoretical Acoustics McGraw-Hill Chap9 1968
24. Thorne P.D. J Acoust Soc Am. 78(3) 1013-1023 Sept. 1985
25. Beranek L.L. McGraw-Hill Chap2. 1971.
26. Love A.E.D. A Treatise on the Mathematical Theory of Elasticity Dover Chap12 1944.
27. Lord Rayleigh Phil Mag. Ser 6, 11 283-291 1906.
28. Junger M.C. etal J Acoust Soc Am 31 978-986 1965.
29. Akay A. etal J Acoust Soc Am 63(2) 313-319 Feb 1978
30. Banerji Phil Mag Ser 6 32, 96-111 July 1916.

31. Akay A. etal Applied Acoustics 11 285-304 1978.
32. Koss L.L. etal J Sound and Vibration 27(1) 59-75 1973.
33. Koss L.L. J Sound and Vibration 36(4) 541-553 1974.
34. Kirchoff G. Mechanick 316-320 1883.
35. Goldsmith. Impact Edward Arnold Chap4 1960.
36. Richards E.J. etal J. Sound and Vibration 62(4) 547-575, 1979.
37. Richards E.J. etal J. South and Vibration 90(1) 59-80, 1983.
38. Holmes A.T. etal J. South and Vibration 51(1) 139-142, 1977.
39. Dyer K.R. NEWC Publ Ser C. 22: 20-24 1980.
40. Langhorne D.N. Institute of Oceanographic Sciences Report No140, pp65 1982.
41. Thorne P.D. etal Marine Geology 54 M43-M48 1984.
42. Thorne P.D. Marine Geology. In Press. 1986.
43. Heathershaw etal Nature Vol.316, No.6026 339-342 25 July 1985.
44. Shield A. Mitt Preuss Versuchsanst fur Wasserbau und Shiffbau Berlin 1963.
45. von-Karman T. Proc of the National Academy of Sciences Washington, V34, 539-565 1948.
46. Hammond F.D.C. etal Sedimentology 31, 51-62, 1984.
47. Miller M.C. Sedimentology 24, 507-527 1977.
48. Thorne. J. Acoust Soc Amer. In Press 1986.

ACOUSTIC TECHNIQUES FOR UNDERWATER SEDIMENT TRANSPORT STUDIES

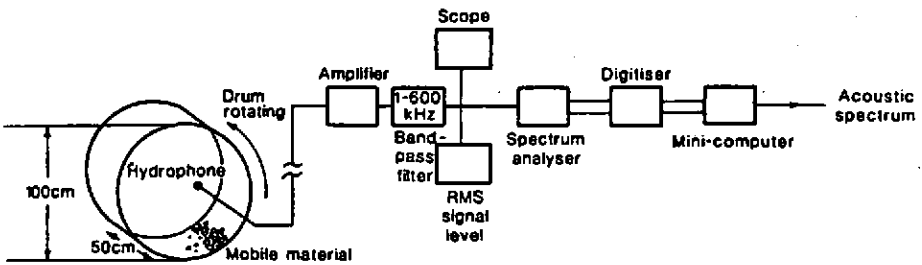

Fig 1: Laboratory instrumentation

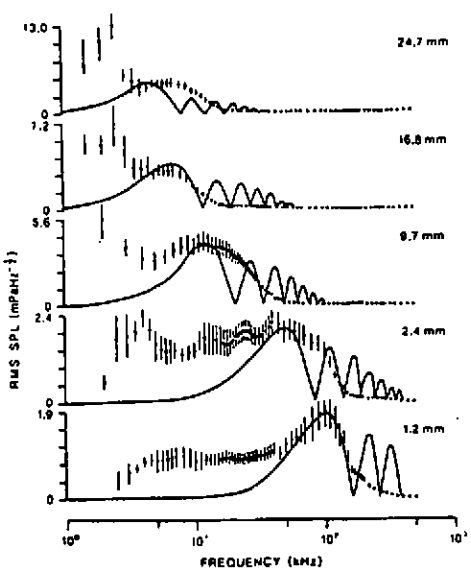

Fig 2: Spectrum variation with particle diameter.— Fourier transform of equation 8.

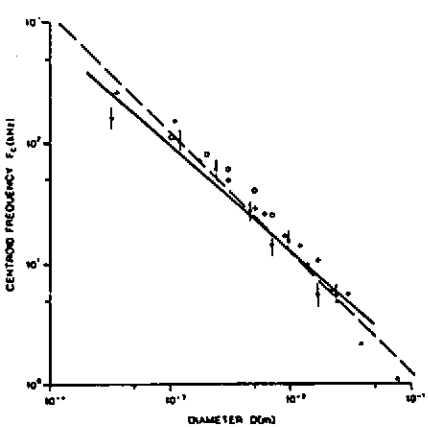

Fig 3: Centroid frequency versus particle diameter. ∮ Present measurement. Other ref's. △14, ○18, ✦24. --- equation 10

ACOUSTIC TECHNIQUES FOR UNDERWATER SEDIMENT TRANSPORT STUDIES

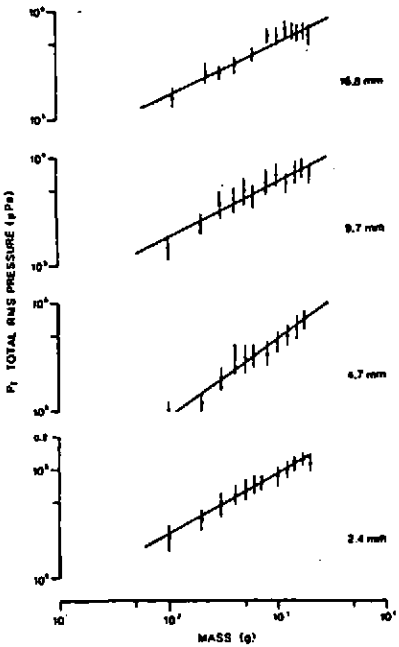

Fig 4: Total pressure variation with mass.

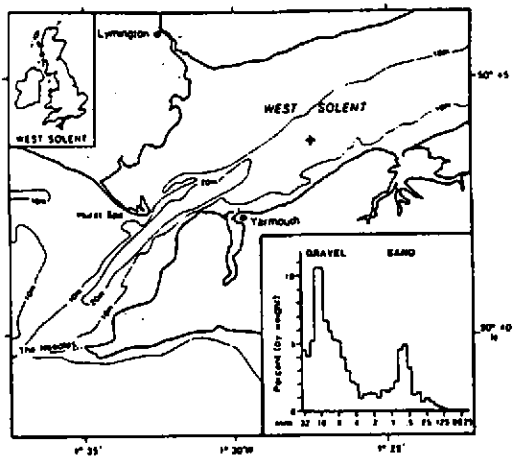

Fig 5: + Location for marine study

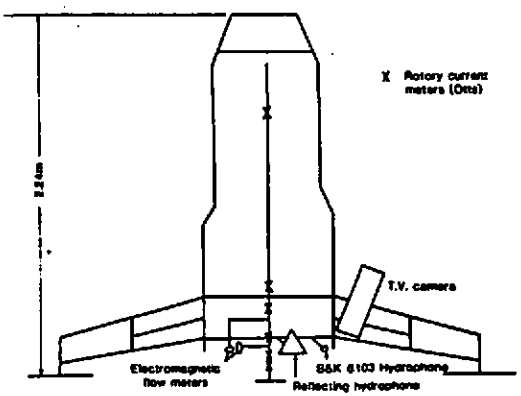

Fig 6: Instrumented rig deployed onto the seabed

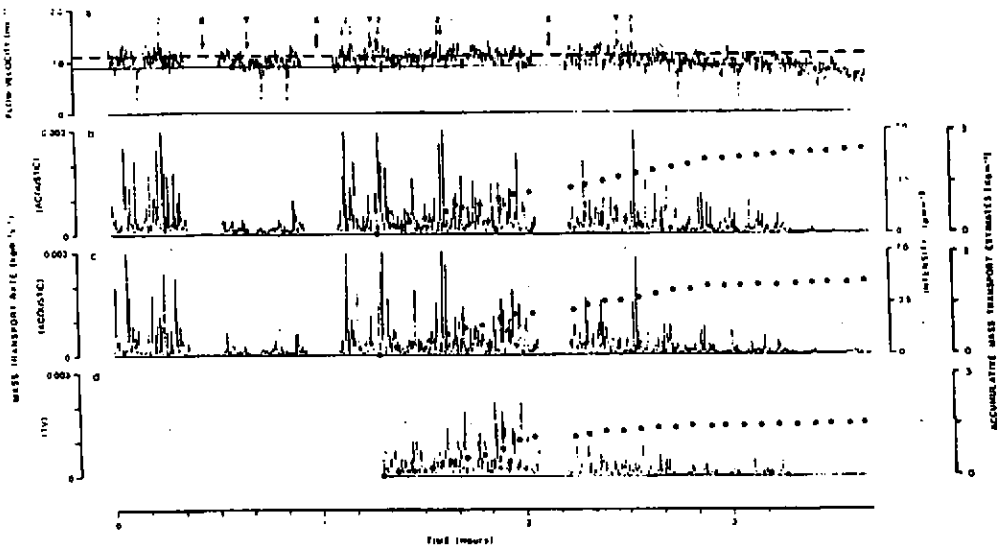

Fig 7: Time series plots. a) Flow velocity, b),c) SGN data, d) T.V. data . accumulative mass transport. --- SGN estimated threshold for sediment transport. —— Threshold from Ref 56.
X Rig repositioned. Y Data breaks. 1. Flow peaks.
2. Flow reductions.

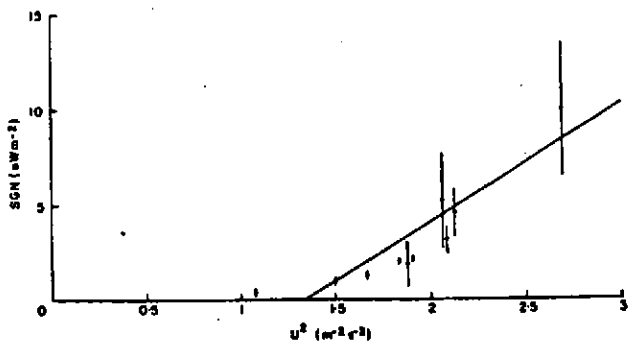

Fig 8: Acoustic measurement for the onset of gravel transport.

ACOUSTIC TECHNIQUES FOR UNDERWATER SEDIMENT TRANSPORT STUDIES

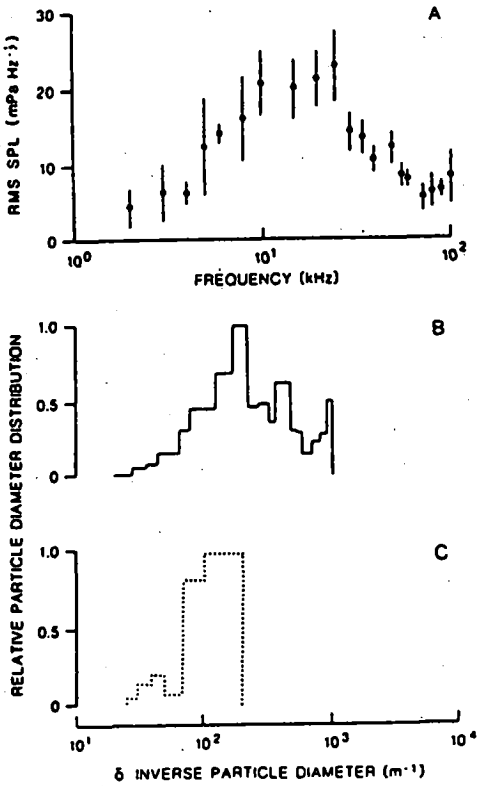

Fig 9: a) In-situ measurement of SGN spectrum for mobile gravel material.
b) SGN estimate of mobile particle size distribution using data in Fig 9a)
c) Visual estimate of mobile particle size distribution.